 DOI: 10.1002/eji.201142086 Eur. J. Immunol. 2012. 42: 936–945

European Journal of Immunology

Targeting of macrophage galactose-type C-type lectin (MGL) induces DC signaling and activation

Chiara Napoletano[*1], *Ilaria G. Zizzari*[*1], *Aurelia Rughetti*[1], *Hassan Rahimi*[1], *Tatsuro Irimura*[2], *Henrik Clausen*[3], *Hans H. Wandall*[3], *Francesca Belleudi*[4], *Filippo Bellati*[5], *Luca Pierelli*[1], *Luigi Frati*[1] *and Marianna Nuti*[1]

[1] Department of Experimental Medicine, "Sapienza" University, Rome, Italy
[2] Graduate School of Pharmaceutical Sciences, University of Tokyo, Tokyo, Japan
[3] Center for Glycomics, Department of Cellular and Molecular Medicine and School of Dentistry, University of Copenhagen, Copenhagen, Denmark
[4] Department of Molecular Medicine, "Sapienza" University, Rome, Italy
[5] Department of Obstetrics and Gynecology, "Sapienza" University, Rome, Italy

Dendritic cells (DCs) sense the microenvironment through several types of receptors recognizing pathogen-associated molecular patterns. In particular, C-type lectins, expressed by distinct subsets of DCs, recognize and internalize specific carbohydrate antigen in a Ca^{2+}-dependent manner. Targeting of these receptors is becoming an efficient strategy of delivering antigens in DC-based anticancer immunotherapy. Here we investigated the role of the macrophage galactose type C-lectin receptor (MGL), expressed by immature DCs (iDCs), as a molecular target for α-N-acetylgalactosamine (GalNAc or Tn)-carrying tumor-associated antigens to improve DC performance. MGL expressed by ex vivo-generated iDCs from healthy donors was engaged by a 60-mer $MUC1_{9Tn}$-glycopeptide as a Tn-carrying tumor-associated antigen, and an anti-MGL antibody, as a specific MGL binder. We demonstrated that MGL engagement induced homotrimers and homodimers, triggering the phosphorylation of extracellular signal-regulated kinase 1,2 (ERK1,2) and nuclear factor-κB activation. Analysis of DC phenotype and function demonstrated that MGL engagement improved DC performance as antigen-presenting cells, promoting the upregulation of maturation markers, a decrease in phagocytosis, an enhancement of motility, and most importantly an increase in antigen-specific $CD8^+$ T-cell activation. These results demonstrate that the targeting of MGL receptor on human DCs has an adjuvant effect and that this strategy can be used to design novel anticancer vaccines.

Keywords: C-type lectins · Dendritic cells · Macrophage galactose-type C-type lectin (MGL) · MUC1 · Tn-tumor associated antigens

Introduction

Dendritic cells (DCs), as professional antigen-presenting cells (APCs), sense the microenvironment through different types of receptors to scan local environmental changes and eliminate incoming pathogens [1]. They play an essential role in the uptake of self- or pathogen-associated antigens, thus, steering and directing the immune response. After activation, DCs migrate to the draining lymph nodes, where they initiate specific immunity

Correspondence: Prof. Marianna Nuti
e-mail: marianna.nuti@uniroma1.it

*These authors contributed equally to this work.

[2]. DCs are equipped with several highly specialized receptors including C-type lectin receptors (CLRs) and Toll-like receptors (TLRs). In contrast to TLRs, CLRs recognize and internalize specific carbohydrate antigens in Ca^{2+}-dependent manner [3], thus, influencing the outcome of the immune response. The most important molecules from the CLR family include macrophage galactose type C-lectin (MGL), dendritic cell-specific intercellular adhesion molecule-3-grabbing non-integrin (DC-SIGN), the mannose receptor, DEC205, and Dectin-1. These receptors are able to trigger distinct signaling pathways that modulate DC functions through the expression of specific molecules and cytokines, determining the polarization of T cells [4]. These properties make this C-type lectin family an optimal tool for DC targeting in cancer vaccination.

Human MGL (hMGL) is a type II C-type lectin, expressed in vitro by macrophages and monocyte derived DCs and in vivo by DCs of skin and lymph nodes [5, 6]. Its carbohydrate recognition domains contain a QPD sequence that is responsible for recognition of α- or β-*N*-acetylgalactosamine (GalNAc, Tn) residues of *N*- and *O*-glycans carried by glycoproteins and/or glycosphingolipids [7]. In mice, there are two homologs of hMGL, MGL1 and MGL2 [8], expressed by dermal DCs and alternatively activated macrophages [5, 9]. MGL1 is highly specific for Lewis X and Lewis A structures, while MGL2, similar to the hMGL, recognizes *N*-GalNAc and galactose, including *O*-linked Tn-antigen, TF-antigen, and core 2 structures [10]. hMGL is equipped with a partial dileucine zipper and with YENF internalization motifs [11]. This receptor is involved in the recognition of a large plethora of pathogens by DCs [12–15] and in the maintenance of T-cell homeostasis [16]. Moreover, in vivo, MGL appears to play a crucial role in close proximity of the endothelial structures of lymph nodes and thymus, where iDCs are hampered in their migration activity until maturation [6]. In cancer, MGL has been described to enable DCs to sense glycosylation [17] and to selectively recognize tumor-associated glycoproteins [18]. The Tn-MUC1 glycoform represents one of the tumor-associated antigens (TAAs) studied as an MGL ligand. MUC1 is a transmembrane epithelial mucin made up of a repeated stretch of 20 amino acid tandem repeated (TR) sequence with several sites of attachment for *O*-linked glycans [19]. In tumors, MUC1 is overexpressed, aberrantly glycosylated, and shed in the tissue microenvironment. MUC1-TAAs carry shortened *O*-glycans such as GalNAcα1-*O*-Ser/Thr (Tn) or Galβ1–3GalNAcα1-*O*-Ser/Thr (T) which may be sialylated [20]. We previously demonstrated that DCs were able to bind to $MUC1_{9Tn}$ glycopeptide (3TRs corresponding to 60 amino acids carrying nine Tn moles) through MGL and this interaction favored the Tn-antigen processing in human histocompatibility leukocyte Ag (HLA) class I and II compartments [18], suggesting its potential application in ex vivo DC-based vaccination.

In this work, we have investigated the effects of MGL targeting on the phenotype and function of ex vivo-generated DC populations, in order to understand whether this receptor could be used as molecular target to activate a potent $CD8^+$ T-cell activation for cell therapy. The ligands chosen for this study were the $MUC1_{9Tn}$ peptide as a model of a Tn-carrying TAA and an anti-MGL antibody as a specific MGL binder. The results demonstrate that MGL activated by both ligands oligomerizes and subsequently activates the extracellular signal-regulated kinase 1,2 (ERK1,2) and nuclear factor-κB (NF-κB) pathways and induces phenotypic and functional DC maturation that then enables the DCs to initiate a strong $CD8^+$ T-cell immune response.

Results

MGL oligomerized and activated the ERK1,2 and NF-κB pathways

Immunofluorescence experiments were conducted to visualize MGL expression changes following receptor engagement. MGL was heterogeneously distributed in iDC population and its localization appeared diffuse on the plasma membrane (Fig. 1A—before). After the addition of $MUC1_{9Tn}$ peptide to iDCs, MGL clustered and its distribution became spotted (Fig. 1A—after). To characterize the receptor complex generated after engagement, MGL clusters were immunoprecipitated and analyzed by western blotting in reducing and non-reducing conditions (Fig. 1B). Two different MGL ligands were used for oligomerization studies: $MUC1_{9Tn}$ as natural ligand and an anti-hMGL monoclonal antibody (MoAb) as specific MGL binder. When the glycopeptide was added to iDCs, MGL clustered as homotrimers and homodimers. In absence of β-mercaptoethanol, two bands corresponding to ∼120 kDa (trimers) and ∼80 kDa (dimers) were found, while a unique band corresponding to MGL monomer (∼40 kDa) was observed in reducing condition (Fig. 1B, on the left).

Similar results were obtained when the anti-MGL antibody was used (Fig. 1B, on the right). After MGL engagement and cross-linking, two bands appeared at ∼420 kDa and ∼230 kDa, corresponding to immunocomplexes containing three and two MGL molecules. In reducing condition, two bands corresponding to MGL monomers and MoAb fragments were detected.

Receptor clustering is usually associated with the activation of intracellular signaling. In order to investigate whether MGL engagement triggers DC intracellular pathways, we analyzed the tyrosine phosphorylation cascades induced by both ligands at different time points. DC lysates were probed with an anti-pTyrosine antibody in western blotting analysis (Fig. 1C). iDCs and iDCs treated with IgG_1 antibody (IgG_1-DCs) were used as negative controls. Results indicate that both $MUC1_{9Tn}$ and the anti-MGL MoAb induced phosphorylation of proteins with an apparent molecular weight ranging between 42 and 44 kDa, suggesting that ERK1,2 could be an optimal candidate substrate protein. When the samples were analyzed with a specific anti-pERK1,2 antibody, we observed that MGL engagement promoted the phosphorylation of ERK1,2. $MUC1_{9Tn}$ appeared to trigger a stronger signal compared with the antibody: bands were visible at 5 min and disappeared after 60 min. The anti-MGL antibody activated a weak phosphorylation signal that was detectable from 5 min, increased becoming more intense at 15 min, and turned off at 60 min.

DC signaling through pattern-recognition receptors is frequently related to the NF-κB pathway [21]. The classical

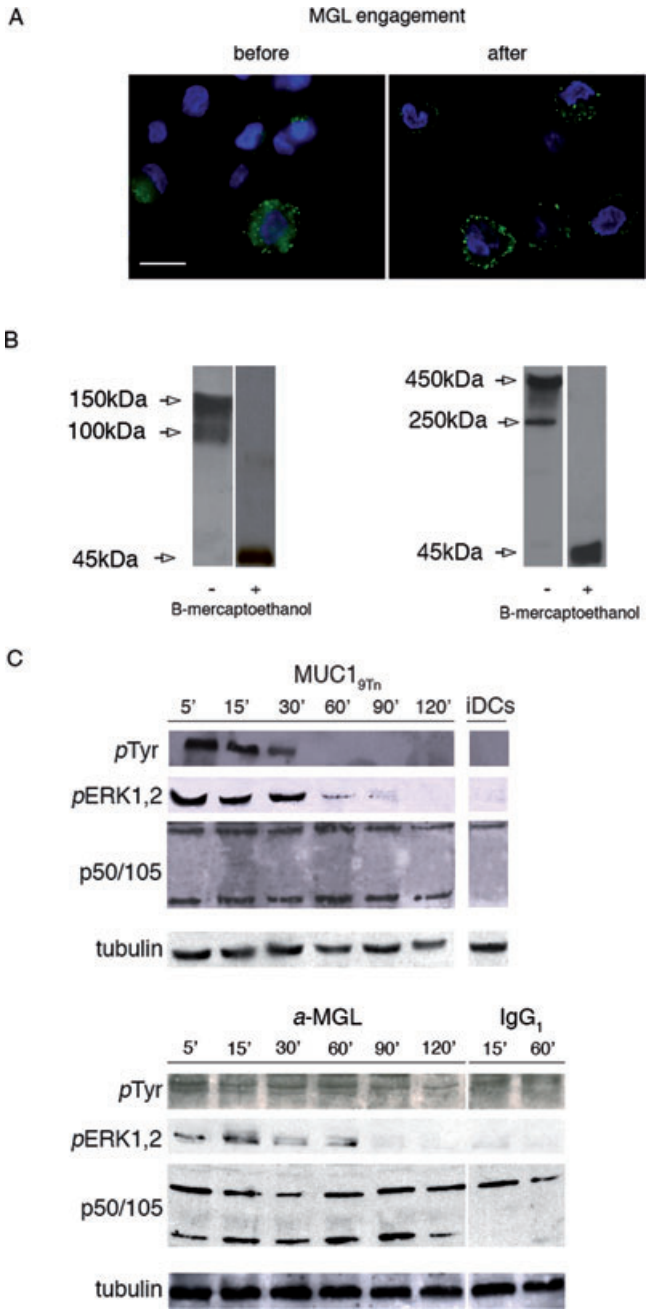

Figure 1. MGL clusters in trimers and dimers and triggers ERK1,2 and NF-κB signals. (A) Fluorescence microscopy of iDCs before and after MGL engagement by $MUC1_{9Tn}$ is shown. MGL is visualized in green, while the nucleus is in blue. Magnification 60×, bar 10 μm. (B) Western blotting analysis of immunoprecipitated MGL after binding and cross-linking to $MUC1_{9Tn}$ peptide (left) and to anti-MGL antibody (right) is shown. Samples were run in 4–12% or 3–8% SDS-PAGE gels and were analyzed in reducing and nonreducing conditions. (C) Western blotting of DC lysates alone or after the addition of $MUC1_{9Tn}$ peptide (left), anti-MGL, and IgG_1 antibodies (right). Samples were analyzed for tyrosine phosphorylation (pTyr), pERK1,2 (42–44 kDa), and for the presence of p50/p105 molecules at different time points. α-tubulin was used as a loading control. Proteins were resolved in 10% SDS-PAGE gel. These results are representative of one donor out of three.

NF-κB signal is dependent on the production of p50-activated form derived from the cleavage of the inactive p105 molecule [22]. Results indicated that MGL engagement by both ligands induced NF-κB activation with a similar pattern; in fact p50 is detectable at 5 min and is maintained after 120 min (Fig. 1C).

DCs matured after MGL activation

Due to the opposite role of ERK1,2 and NF-κB signaling on DC maturation [23, 24], we next evaluated the effects of MGL activation on phenotype and functions of DCs. We studied the expression of several DC markers after MGL binding, comparing the results with those obtained with iDCs or IgG_1-DCs (Fig. 2). DCs matured with interleukin (IL)-1β, IL-6, tumor necrosis factor-α (TNF-α), and prostaglandin E_2 were used as positive control. DCs derived from six healthy donors were characterized for the expression of HLAII-DR, HLAI, CD86, CD83, CD40, CCR7, intercellular adhesion molecule (ICAM-1), CD11c, and CD1a molecules. After MGL engagement, DCs were left overnight at 37°C to allow phenotype marker modulation. Results indicated that both MGL ligands induced DC maturation, although at different extent. The glycoimmunogen $MUC1_{9Tn}$ modified DC phenotype, significantly increasing the expression of HLAII-DR, CD83, and CD40 molecules compared with that of iDCs. The average values of mean fluorescence intensity (MFI) obtained for CCR7, CD11c, and CD1a highlighted a trend in the upregulation of these markers, although these modifications were not statistically significant.

The anti-MGL antibody promoted a significant upregulation of HLAII-DR, CD86, CD83, CCR7, and CD40 compared with IgG_1-DCs, while the other DC markers appeared unmodified.

MGL engagement enhanced DC motility and reduced DC endocytosis

iDCs display an enhanced ability to capture and process pathogens, while showing a strongly reduced motility [25]. The exposure to maturation stimuli induces functional changes including down regulation of endocytic capacity and increased migration ability enabling DCs to move to lymph nodes where they present antigen to T cells. Thus, the endocytic capacity of DCs treated with $MUC1_{9Tn}$ peptide ($MUC1_{9Tn}$-DCs) and with the anti-MGL antibody (a-MGL-DCs) was evaluated by fluorescein isothiocyanate (FITC)-dextran uptake and analyzed by flow cytometry (Fig. 3A). Both ligands induced a reduction in endocytosis: this decrease corresponded to 38% when the glycopeptide was used for MGL activation (iDCs versus $MUC1_{9Tn}$-DCs: 15.4 versus 9.6) and to 56% with the antibody (IgG_1-DCs versus a-MGL-DCs: 14.5 versus 6.4).

Moreover, MGL engagement enhanced migratory capacity of DCs, in fact as expected by the upregulation of CCR7 induced by the anti-MGL antibody and in a less pronounced manner by $MUC1_{9Tn}$, a discrete DC population acquired the capacity to migrate toward CCL19 (16 ± 3% for the antibody; 9 ± 4% for $MUC1_{9Tn}$ peptide; Fig. 3B).

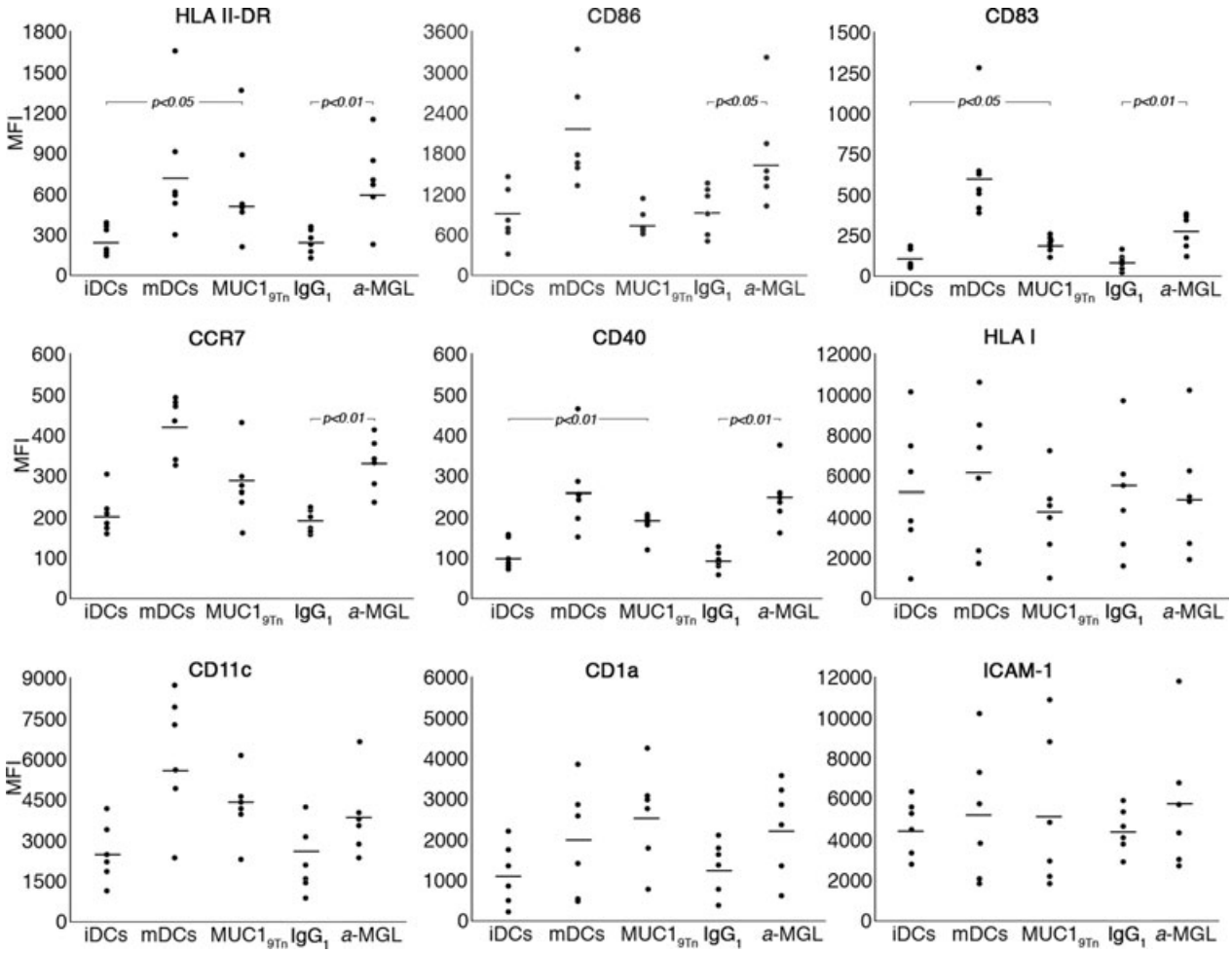

Figure 2. MGL engagement induces DC maturation. The MFI values of DC phenotypic markers derived from six healthy donors at day 5 of culture are shown. The cells were treated with MUC1$_{9Tn}$ peptide (10 μg/mL) for 1 h on ice and with anti-MGL (10 μg/mL) or IgG$_1$ antibodies for 30 min on ice. DCs were then washed and incubated at 37°C overnight before analysis. iDCs and mDCs (IL-1β, IL-6, TNF-α, and PGE$_2$) were used as negative and positive controls, while IgG$_1$ represents the isotype control of the anti-MGL antibody. The bars correspond to the average MFI values among six donors. Statistical significance was determined by the Student's paired *t*-test.

MGL activation decreased IL-10 production of DCs

IL-12 and IL-10 are two cytokines, produced by DCs, involved in the regulation and balancing of the immune response, respectively, representing two important parameters to understand the type of immune response evoked [26]. We evaluated the percentage of IL-12 and IL-10 produced by MGL-engaged DCs by intracellular staining (Fig. 3C). DCs treated with the anti-MGL antibody showed a percentage of IL-12 producing cells significantly higher compared with IL-10$^+$ cells ($p < 0.05$), thus showing a shift in the IL12/IL10 balance toward a Th1 polarization, as observed in mature DCs (mDCs) ($p < 0.01$). Such shift was not detectable in the other experimental conditions.

MGL-activated DCs induced allogeneic T-cell proliferation

In order to understand the effects of MGL-induced DC maturation on T-cell response, we analyzed the capacity of MUC1$_{9Tn}$-DCs and a-MGL-DCs to stimulate the proliferation of allogeneic T cells. Lymphocyte proliferation was evaluated after 5 days of DCs: T cells were cocultured at different ratios, measuring the incorporation of ^{3}H-thymidine (Fig. 4A). The results showed that MUC1$_{9Tn}$ induced a similar T-cell proliferation to that exerted by iDCs. On the other hand, a-MGL-DCs activated a strong T-cell proliferative response, comparable to that induced by mDCs when used at 1:5 and 1:10 ratio. This capacity was significantly higher than those displayed by IgG$_1$-DCs, iDCs, and MUC1$_{9Tn}$-DCs.

MGL-engaged DCs stimulated IFN-γ production by autologous antigen-specific CD8$^+$ T cells

We finally studied the effect of MGL engagement on the capacity of DCs to activate a CD8$^+$ T-cell mediated antigen-specific response (Fig. 4B). CD8$^+$ T cells, obtained from three HLAI-A2$^+$ healthy donors, were stimulated with autologous iDCs, mDCs, IgG$_1$-DCs, MUC1$_{9Tn}$-DCs, and a-MGL-DCs pulsed with HLAI-A2

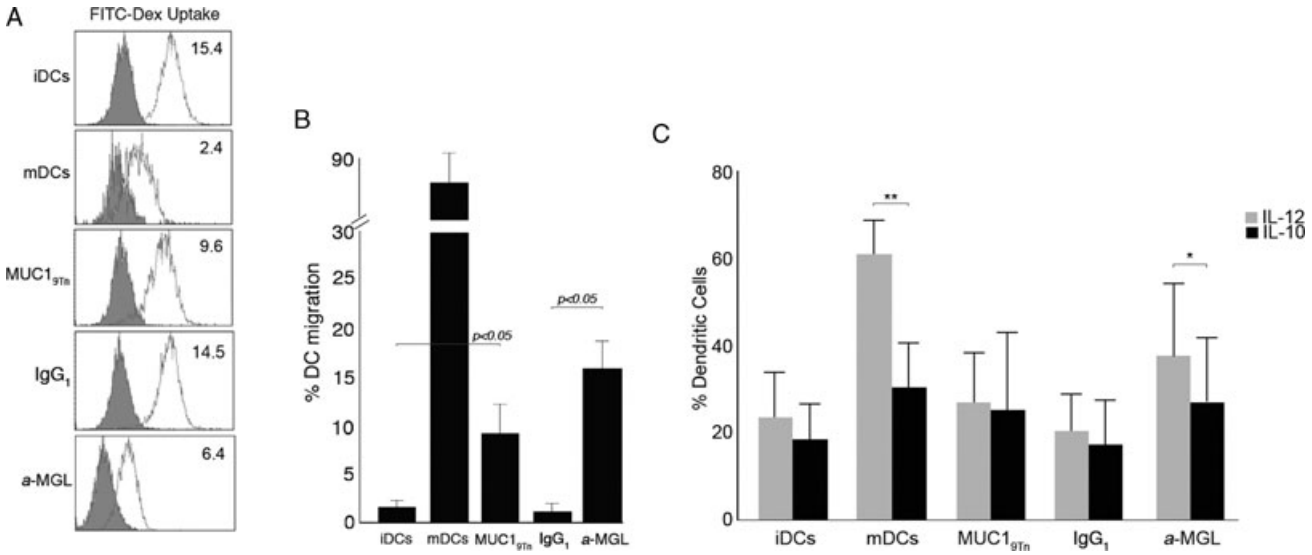

Figure 3. MGL activation decreases DC endocytosis, increases DC migration, and decreases the production of IL-10. (A) The endocytic capacity of iDCs, mDCs, IgG_1-DCs, $MUC1_{9Tn}$-DCs, and a-MGL-DCs was evaluated as FITC-dextran uptake (1mg/mL/10^6 cells). Open histograms represent the dextran uptake obtained after 2 h at 37°C, while filled histograms show the dextran endocytosis after 2 h at 4°C (negative control). The values reported on the top of each histogram indicate the ratio between MFI of positive and negative samples. Results are representative of one donor out of six (B) The percent migration of iDCs, mDCs, IgG_1-DCs, $MUC1_{9Tn}$-DCs, and a-MGL-DCs toward CCL19 was determined in 24-well Transwell cell culture chambers (90 min, 37°C). The results correspond to the mean + SD (standard deviation) of six donors. (C) Intracellular cytokine staining of IL-12 and IL-10 was performed in differently activated DCs. Gray columns represent the percentage of IL-12 producing DCs, while the black columns correspond to the percentage of IL-10 producing cells. The results correspond to the mean + SD of six donors. $^*p < 0.05$, $^{**}p < 0.01$, Student's *t*-test.

restricted Flu peptide (GILGFVFTL). $CD8^+$ T-cell activation was measured as Interferon (IFN)-γ production in enzyme-linked immunospot (ELISpot) assay. Results indicated that MGL-stimulated DCs, both by $MUC1_{9Tn}$ and anti-MGL antibody ligands, were optimal APCs able to induce a strong IFN-γ $CD8^+$ T-cell response similarly to mDCs, while the IFN-γ response activated by iDCs was significantly lower.

Discussion

In the last years, the immunological potential of DCs has been proposed as a basic formula for cancer vaccines. Several clinical trials are currently ongoing worldwide to validate the efficacy of this cellular immunotherapy utilizing ex vivo generated DCs pulsed with a variety of TAAs in different formulations such as tumor lysate and peptides [27]. The optimal targeting of DCs to induce specific anticancer immune activation is however still matter of investigation. The targeting of CLRs on DCs has recently acquired a great interest for cancer immunotherapy. Several authors have recently demonstrated that CLR targeting represents an optimal strategy to enhance antigen presentation by DCs, because CLRs are the designed receptors that can recognize endocytose glycans expressed by TAAs released during tumor progression [10, 17, 18]. Different approaches have been proposed to target CLRs in vivo and in vitro, such as antigen coupling to CLR-specific antibody and recombinant glycoproteins [28].

MGL receptor belongs to the CLR family and it has recently been shown in mouse models that MGL-targeted DCs modulate the immune response. The targeting of MGL expressed by dermal DCs induced a strong HLA class II-restricted T-cell response with a concomitant induction of a potent anti-Tn antibody response following the internalization of MAG:Tn3 glycoimmunogen, containing a viral $CD4^+$ T-cell epitope [29]. Moreover, MGL enhanced both $CD4^+$ and $CD8^+$-T lymphocyte activity in TLR independent manner when interacted with Tn-OVA (ovalbumin) antigen [30]. Tn-polyacrylamide polymers conjugated to streptavidin were efficiently internalized through MGL and primed streptavidin-specific $CD4^+$ T cells [31]. Our previous study, conducted in human setting, demonstrated that the overall structure of Tn-carrying molecules internalized by this receptor highly influenced the antigen processing. In fact, recombinant Tn-glycoproteins resembling those shed by tumors remained blocked in HLA class II compartment after internalization, while shorter Tn-antigen formulations were processed in HLA class I and II compartments [18].

Since MGL is a strong binder for Tn-carrying molecular structures, such as Tn-TAAs, and is expressed on human DCs during differentiation, we were prompted to further investigate the role of this specific targeting receptor on DC performance, envisaging possible application in cancer vaccines.

We used two different types of ligands: an anti-MGL antibody as a classical model of specific receptor binder and $MUC1_{9Tn}$ peptide as Tn-carrying TAA that we previously demonstrated to be cross-processed to HLA class I [18].

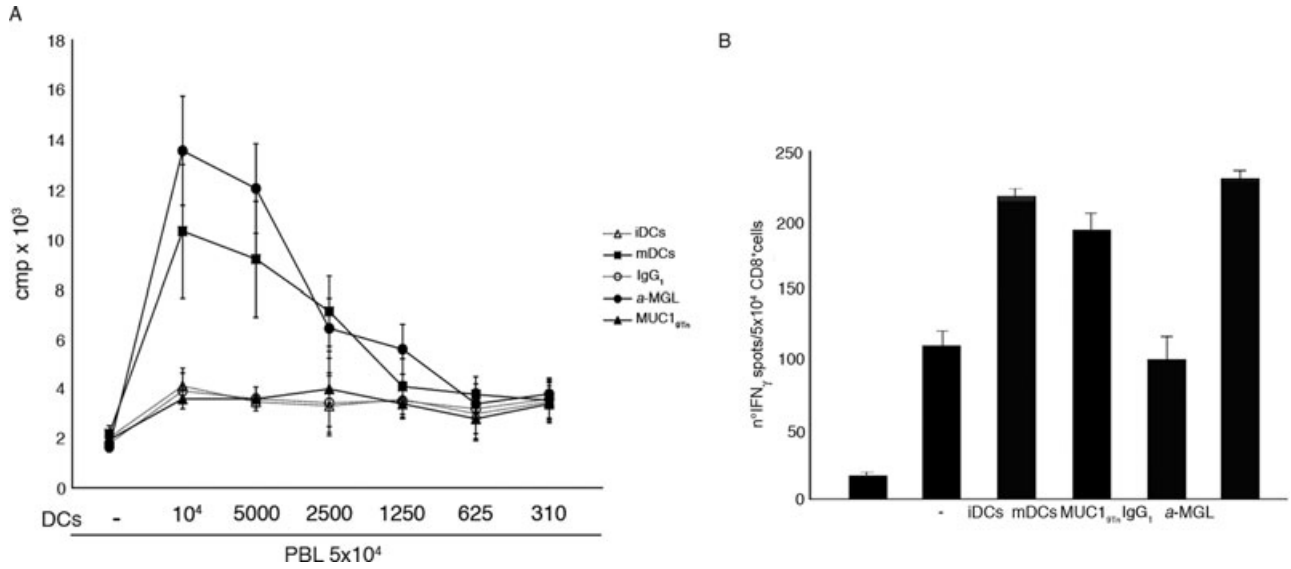

Figure 4. MGL-activated DCs promote the proliferation of allogeneic $CD4^+CD45RA^+$ cells and stimulate $CD8^+$ T cells to produce IFN-γ. (A) A titration of iDCs, mDCs, IgG_1-DCs, $MUC1_{9Tn}$-DCs, and a-MGL-DCs were cocultured with 5×10^4 allogeneic immunoselected $CD4^+$ T lymphocytes. T-cell proliferation was measured as ^{3}H-thymidine incorporation and results were reported as counts per minutes. The results are representative of one donor out of six. (B) The number of IFN-γ spots produced by $CD8^+$ T cells (5×10^4/well) when stimulated with iDCs, mDCs, IgG_1-DCs, $MUC1_{9Tn}$-DCs, and a-MGL-DCs pulsed with Flu peptide are shown. $CD8^+$ T cells plus Flu peptide were used as negative control. The background (DCs plus $CD8^+$ T cells without Flu peptide) was subtracted from each sample. Results correspond to the mean + SD from three donors.

First, we analyzed DC phenotype changes induced by MGL engagement. The glycopeptide $MUC1_{9Tn}$ and the antibody were both able to promote similar, although distinct effects on DCs. In fact, $MUC1_{9Tn}$-DCs showed a significant upregulation of HLAII-DR, CD83, and CD40 and exhibited a trend in the upregulation of CCR7, CD11c, and CD1a. These phenotypic changes were accompanied by a moderate decrease in endocytosis and an increase in the cell motility. When DCs were treated with the anti-MGL antibody, also a significant increase of CD86 and CCR7 was observed in accordance with a more evident endocytosis downregulation and an increment of antigen presenting activity. The effects of the C-type lectin targeting on DCs have been largely investigated by several authors using specific antibodies or antigen-conjugated MoAb. Dectin-1 engagement promoted an increase in the expression of CD86, CD80, CD40, and HLAII-DR [32], while DC-SIGN ligation did not stimulate DC maturation [33]. In other studies, C-type lectin activation resulted in the secretion of multiple cytokines and chemokines by DCs [32, 34, 35], even if the upregulation of costimulatory molecules was not always detected. Moreover, C-type lectin targeting increased DC cross-presentation or improved the activation by DCs of specific lymphocyte subsets [36, 37].

In our system the engagement of MGL by both ligands induced activation of antigen-specific $CD8^+$ T cells as detected by IFN-γ production, while only DCs stimulated with the antibody, induced the proliferation of allogeneic T cells similarly to mDCs. The difference in the profile of costimulatory molecules observed could make account for the distinct immunogenicity. In fact, CD86, that strongly contributes to alloreaction [38], was upregulated only in a-MGL-DCs and not in MUC_{9Tn}-DCs, while upregulation of CD40 was induced by both ligands. The balancing among the expression profile of costimulatory molecules, inhibitory regulators, and the timing of expression on DCs finely tunes the interaction between APCs and the effector T cells. In addition, this DC population was able to switch the balance IL-12/IL-10. In fact, the increase of IL-12 production compared with IL-10 in this DC subset further suggests their capacity to favor a polarization toward a Th1 population.

The shaping of phenotypic and functional performance of DCs after C-type lectin engagement strongly correlates to the triggering of intracellular signaling [4].

We have demonstrated for the first time that MGL oligomerized and triggered the phosphorylation of ERK1,2 and the activation of NF-κB signal. The $MUC1_{9Tn}$ glycoimmunogen and the antibody showed the same ability to induce clusters and to activate the p50 transcription factor, but they acted differently in the triggering of ERK1,2 pathway (stronger activation in $MUC1_{9Tn}$-DCs). It is well known that ERK1,2 pathway profoundly influences DC activity. The effects of ERK1,2 signaling on maturation of DCs are highly variable and dependent on the type of stimulus added to the cells, even if it appears to negatively regulate the phenotypic and functional maturation of DCs [39]. On the other hand, the activation of NF-κB signal is essential for DC development and survival and has a high impact on DC maturation and in the production of proinflammatory cytokines, such as IL-12, IL-6, TNF-α, and IFN-α/β [23, 40]. In our system, two different ligands for the same receptor induced a distinct dynamic and intensity of the ERK1,2 activation and this could make account of the distinct phenotypic and functional performances displayed by $MUC1_{9Tn}$-DCs versus a-MGL-DCs. The choice of the binder for DCs targeting is a crucial step when designing DC cancer vaccines.

CLR-specific antibodies coupled with TAAs have been proposed for the targeting of DCs. However, the efficiency of these binders could be severely hampered by reduced tissue penetration and nonspecific Fc Receptor (FcR)-mediated uptake by other cells. The use of synthetic Tn-TAAs for DC targeting represents a promising approach and our model of glycopeptide, $MUC1_{9Tn}$, represents here the "proof of concept" of this strategy. We believe and speculate that modifying Tn-density, the length and steric structure of the Tn-peptide, we can possibly obtain immunogens that can efficiently bind to MGL, strongly activate DCs, mimic the effects of a danger signal, and achieve an efficient presentation in HLA class I and II pathways as previously described [18]. Moreover, a wide variety of immunogens carrying Tn-epitopes could be envisaged, where the Tn-peptide stretch could only be a way to deliver other TAAs as well as other molecules.

It is also important to retain that the molecular targeting as well as the choice of the antigen represent only "one side of the coin" in designing cancer vaccines. The choice of the optimal DC subset for priming T cells combined to strategies to contain or eliminate immunosuppression are crucial parameters that should be considered to obtain an efficacious and long-lasting anticancer immunoresponse [41].

In conclusion, in this work we have demonstrated that MGL engagement promotes DC activation and that the effects of this activation are strongly dependent on the type of stimulus added to the cells. The high plasticity of MGL and its capacity to modulate the immune response combined to its ability to endocyte and process GalNAc-carrying antigens makes MGL an optimal candidate to be targeted for immunotherapy.

Materials and methods

DC generation

Peripheral blood mononuclear cells were isolated by Ficoll-Hypaque gradient (1077 g/mL; Pharmacia LKB, Uppsala, Sweden). Monocytes ($CD14^+$) were purified by CD14 MicroBeads (Miltenyi Biotech, Paris, France) and cultured (5×10^5 cells/mL) in RPMI 1640 (Hyclone, UT, USA) supplemented with 2 mM L-glutamine (Sigma Chemical Company, St. Louis, MO, USA), penicillin 100 U/mL (Sigma), streptomycin 100 μg/mL (Sigma) with 10% heat-inactivated Fetal Calf Serum (Hyclone). A total of 50 ng/mL rhGranulocyte-Macrophage colony-stimulating factor (R&D System, Minneapolis, MN) and 1000 U/mL rhIL-4 (R&D System) were added at day 0. iDCs were collected at day 5 and matured with rhIL-1β (10 ng/mL), IL-6 (10 ng/mL), TNF-α (10 ng/mL), and prostaglandin E2 (1 μg/mL) (all purchased by R&D System) for 16 h. At day 6 DCs were considered matured.

Chemoenzymatic synthesis of glycopeptides

Unglycosylated MUC1–60-mer peptide (VTSAPDTRPAPGST APPAHG)$_{n=3}$ representing 3TRs was synthesized by Neosystem, Prague, Czech Republic) as described by Fontenot et al. [42]. Recombinant human polypeptide GalNAc-transferase GalNAc-T2, was used to direct GalNAc *O*-glycosylation of MUC1 peptides at three sites per TR ($MUC1_{9Tn}$) as previously described [43]. Glycosylation was controlled using nanoscale reversed-phase columns (Poros R3, PerSeptive Biosystems, Framingham, MA, USA) and MALDI-TOF mass spectrometry.

Flow cytometry

Cell phenotype staining was performed using the following antibodies: MoAbs anti-hMGL (ASGPR/MGL, 125A10.03 clone, Dendritics, Lyon, France) and anti-HLAI (W6/32 clone) (Sigma) followed by FITC-conjugated goat anti-mouse IgG (H + L) (Jackson ImmunoResearch Laboratories, West Grove, PA, USA). MoAbs directly conjugated with FITC or phycoerythrin (PE) were also employed: IgG_1 or IgG_{2b} or IgG_{2a}-FITC and IgG_1 or IgG_{2b}-PE as isotype controls, anti-HLAII-DR-FITC (IgG_{2b}), anti-CD86-FITC (IgG_1), anti-CD83-PE (IgG_1), anti-CD40-PE (IgG_1), anti-CD11c-PE (IgG_{2b}), anti-CD54-PE (ICAM-1) (IgG_1), and anti-CD1a-PE (IgG_1) all from Becton Dickinson (San Diego, CA, USA) and anti-CCR7-FITC (IgG_{2a}) from R&D. DCs were incubated with conjugated-MoAb for 30 min at room temperature (RT) as indicated by the manufacturer's instruction. After washing, least 1×10^4 events were evaluated using a FACSCanto flow cytometer running FACS-Diva data acquisition and analysis software (Becton Dickinson).

Confocal microscopy

To study the MGL distribution on DC plasma membrane, iDCs (1×10^6/sample) were fixed with 4% paraformaldehyde (Electrom Microscopy Science, Hatfield, PA, USA) for 30 min, followed by glycine 0.1 M (Sigma-Aldrich, San Luis, USA) for 10 min and 0.1% Triton-X-100 (Bio-Rad Laboratories, CA, USA) for 4 min. iDCs were incubated with MoAb anti-MGL (Dendritics) for 45 min, and then with goat anti-mouse-FITC $F(ab')_2$ antibody. Cells were added on to SuperFrost®PlusMicroscope Slides (Menzel-Glaser, Germany) after the addition of Mowiol mounting medium (Calbiochem, Darmstadt, Germany). To visualize the MGL distribution after the receptor engagement, iDCs were treated with $MUC1_{9Tn}$ glycopeptide and next incubated with MoAb anti-MGL (Dendritics) followed by goat anti-mouse-FITC $F(ab')_2$ antibody. Cells were then fixed and scanned in a series of 0.5-μm sequential sections with an ApoTome System (Zeiss, Ober Kochen, Germany) connected with an Axiovert 200 inverted microscope (Zeiss); image analysis was then performed by the Axiovision software (Zeiss), and a three-dimensional reconstruction was obtained.

MGL oligomerization and immunoprecipitation

A total of 5×10^6 DCs were incubated with $MUC1_{9Tn}$ peptide (10 μg/mL) or with MoAb anti-MGL (Dendritics) for 1 h and

30 min, respectively, on ice. Cells were washed and treated with 1 mM BS^3 cross-linker (Calbiochem, Darmstadt, Germany) for 30 min at RT. A total of 10 mM Tris-HCl was then added for 15 min at RT. After washing, Nonidet P-40 (NP-40) solution (Biocompare, San Francisco, CA) (200 μL) with phenylmethylsulfonyl fluoride (1 mM) (Sigma) and protease inhibitors (1X) (Sigma) were added to the cells for lysis for 30 min on ice. The cellular suspension was centrifuged at 13,000 × *g* for 10 min at 4°C and the supernatant was collected.

MGL immunoprecipitation was performed using the Immunoprecipitation Kit-–Dynabeads Protein G (Invitrogen, Oslo, Norway) according to manufacturer's instruction. Briefly, 50 μL of Dynabeads-protein G were added to 5 μg of MoAb anti-MGL (Dendritics) in 200 μL of Ab Binding & Washing Buffer for 15 min at RT. MGL antibody-coated beads were then washed and added to the cellular supernatant derived from $MUC1_{9Tn}$-DCs, overnight at 4°C. Supernatants derived from a-MGL-DCs were directly incubated with 50 μL of Dynabeads-protein G protein coated to normal goat anti-mouse IgG (Santa Cruz, CA, USA) for 16 h at 4°C. The receptor coated to beads was magnetically isolated and eluted using 20 μL of Elution Buffer. The concentration of eluted samples was evaluated using the Bradford assay (Bio Rad, München, Germany).

MGL engagement

iDCs (10^6 cells/mL) derived from six healthy donors at day 5 of culture were treated with phosphate-buffered saline (PBS) + 10% FCS for 30 min to reduce the unspecific binding sites. The cells were then incubated with IgG_1 (Sigma) (10 μg/mL) or anti-MGL antibodies (10 μg/mL) (Dendritics) for 30 min on ice or with $MUC1_{9Tn}$ peptide (10 μg/mL) for 1 h on ice. Optimal incubation time was defined by oligomerization results. Cells were then washed to remove ligands and incubated for 16 h at 37°C. iDCs were used as negative controls in all experiments.

Western blotting

For oligomerization studies, immunoprecipitated samples were subjected to 3–8% or 4–12% sodium dodecyl sulfate-polyacrylamide gel electrophoresis (SDS-PAGE) and the resolved proteins were transferred electrophoretically to nitrocellulose transfer membrane (Schleicher and Schuell, Dassel, Germany). The unspecific sites were blocked with phosphate-buffered saline + 5% bovine serum albumin (BSA) (Sigma) overnight at 4°C. Nitrocellulose membrane was then incubated with MoAb anti-MGL (Dendritics) (1:10) overnight at 4°C followed by peroxidase-conjugated goat anti-mouse IgG (H + L) antibody (1:20,000) (Jackson ImmunoResearch Laboratories, Suffolk, UK) 1 h at RT.

For the signal transduction experiments, iDCs were stimulated with $MUC1_{9Tn}$ peptide or with anti-MGL (Dendritics) and IgG_1 antibodies as described above. Cells were washed and incubated at 37°C from 5 to 120 min. DCs were then lysed using the NP-40 solution (Biocompare) with phenylmethylsulfonyl fluoride (1 mM) (Sigma) and protease inhibitors (1X) (Sigma) and the proteins obtained were resolved using 10% SDS-PAGE and transferred to nitrocellulose. After blocking, membranes were incubated with mouse anti-phosphotyrosine (4G10 clone, Millipore, Billerica, MA, USA) (1:1000), mouse anti-phospho-p44/42 (E10 clone, Cell Signaling Technologies, Boston, MA, USA) (1:1000), rabbit anti-p50 (NLS clone, Santa Cruz, CA, USA) (1:500), and anti-αtubulin (B-7 clone, Santa Cruz) (1:1000) antibodies, followed by peroxidase-conjugated goat anti-mouse or anti-rabbit IgG (H + L) (Jackson ImmunoResearch Laboratories) (1:10,000). For both type of studies, the protein bands were detected with Lite Ablot Extend (Euroclone, Lugano, Switzerland), following the manufacturer's instructions.

Endocytosis

FITC-dextran (1 mg/mL) (Molecular Probes, MoBiTec, Gottingen, Germany) was added to iDCs, mDCs, IgG_1-DCs, a-MGL-DCs, and $MUC1_{9Tn}$-DCs for 2 h at 37°C. After washing, cells were analyzed by flow cytometry using FACSCanto flow cytometer. DCs incubated with FITC-dextran for 2 h at 4°C were used as negative controls.

DC migration

DC migration toward CCL19 (MIP-3β/CCL19 C/F, (R&D Systems) was determined using chemotaxis assay performed in 24-well Transwell cell culture chambers (Corning Costar Corp., NY, USA) containing a 5.0 μm-pore size membrane. The upper chamber was loaded with 1×10^5 iDCs, mDCs, IgG_1-DCs, a-MGL-DCs, and $MUC1_{9Tn}$-DCs. The lower compartment contained 600 μL RPMI 1640 medium, 0.5% BSA (Sigma) and 10 mM N-2-hydroxyethylpiperazine-N′-2-ethanesulfonic acid (Hyclone) with CCL19 (250 ng/mL). After incubation at 37°C for 90 min, cells that had migrated into the lower compartment were collected and the percentage of migration was determined as migrated/total events using FACSCalibur flow cytometer (Becton Dickinson).

DC cytokine production

iDCs, mDCs, IgG_1-DCs, a-MGL-DCs, and $MUC1_{9Tn}$-DCs were stimulated with phorbol myristate acetate (25 ng/mL) (Sigma) and ionomicyn (250 ng/mL) (Sigma) in presence of Brefeldin A (10μg/mL) for 16 h at 37°C. Cells were collected, fixed, and permeabilized with Saponin (Sigma) solution at 0.5%. Intracellular staining was carried out using anti-IL-10-FITC (R&D System) and anti-IL-12-FITC (R&D System) antibodies. Cells were acquired by FACSCanto flow cytometer and analyzed by FACS-Diva software.

Mix lymphocyte reaction

Naïve $CD4^+$ T cells were purified from peripheral blood by Ficoll-Hypaque gradient (1077 g/mL; Pharmacia LKB) followed by CD4 and CD45RA immunomagnetic isolation (Miltenyi Biotech). $CD4^+CD45RA^+$ cells (5×10^4 responder cells/well) were then cocultured in triplicate in a 96 round-bottom microplate (Costar, New York, USA) with decreasing numbers of allogeneic iDC, mDCs, IgG_1-DCs, a-MGL-DCs, and $MUC1_{9Tn}$-DCs irradiated at 3000 rads. Cultures were maintained in a humidified atmosphere at 37°C and 5% CO_2. Thymidine incorporation was measured after 5 days by 16–18 h pulse with ^{3}H-thymidine (1 μCi/well, Amersham, Boston, MD, USA). Evidence of deoxyribonucleic acid incorporation of ^{3}H-thymidine, as an index of cell proliferation, was estimated by harvesting the content of each well onto glass-fiber filters, which were then counted using liquid scintillation counter (Hewlett-Packard Company, Palo Alto, CA, USA). Responses were reported as mean counts per minute of triplicate estimates.

ELISpot

Plates (Millipore, Bedford, MA, USA) were coated with 50 μL of MoAb anti-human IFN-γ (10 μg/mL) (Pharmingen, San Diego, CA, USA) overnight at 4°C. After three washing steps and blocking with phosphate-buffered saline + 1% BSA (Sigma) (200 μL/well, 2 h at 37°C), $CD8^+$ T cells (5×10^4 cells/well) were plated in triplicate with iDCs, mDCs, IgG_1-DCs, a-MGL-DCs, and $MUC1_{9Tn}$-DCs with HLAI-A2 restricted Flu peptide (GILGFVFTL) (10 μg/mL) (Proimmune, Oxford, UK) for 16 h at 37°C. Cells were then removed and after washing, cytokine release was detected with biotinylated anti-IFN-γ antibody (Pharmingen) (5 μg/mL, 50 μL/well, 2 h at RT) revealed with streptavidin-alkaline phosphatase (Pharmingen) (dilution 1:2000, 50 μL/well, 2 h at RT) and chromogen substrate (5-bromo-4-chloro-3-indolylphosphate (BCIP)/nitroblue tetrazolium alkaline phosphatase substrate, Sigma) (50 μL/well). Spots were counted using the ImmunoSpot Image Analyzer (Aelvis, Germany).

Statistical analysis

Descriptive statistics (average and standard deviation) were used to describe the various groups of data. Student's paired *t*-test was used to analyze statistical differences between groups. Significance is indicated when the p value is less than 0.05.

Acknowledgements: This work was supported by Associazione Italiana per la Ricerca sul Cancro (AIRC), Ministero dell'Istruzione, dell'Università e della Ricerca (MIUR), Ricerche Universitarie (ex ATENEO).

Conflict of interest: The authors declare no financial or commercial conflict of interest.

References

1 **van Vliet, S. J., García-Vallejo, J. J. and van Kooyk, Y.**, Dendritic cells and C-type lectin receptors: coupling innate to adaptive immune responses. *Immunol. Cell. Biol.* 2008. **86**: 580–587.

2 **Cummings, R. D. and McEver, R. P.**, C-type Lectins. In Varki, A., Cummings, R. D., Esko, J. D., Freeze, H. H., Stanley, P., Bertozzi, C. R., Hart, G. W. **et al.** (Eds.), *Essentials of glycobiology*, 2nd edition,Cold Spring Harbor Laboratory Press, Cold Spring Harbor, New York, 2009, Chapter 31.

3 **Zelensky, A. N. and Gready, J. E.**, The C-type lectin-like domain superfamily. *FEBS J.* 2005. **272**: 6179–6217.

4 **Geijtenbeek, T. B. and Gringhuis, S. I.**, Signalling through C-type lectin receptors: shaping immune responses. *Nat. Rev. Immunol.* 2009. **9**: 465–479.

5 **Raes, G., Brys, L., Dahal, B. K., Brandt, J., Grooten, J., Brombacher, F., Vanham, G. et al.**, Macrophage galactose-type C-type lectins as novel markers for alternatively activated macrophages elicited by parasitic infections and allergic airway inflammation. *J. Leukoc. Biol.* 2005. **77**: 321–327.

6 **van Vliet, S. J., Paessens, L. C., Broks-van den Berg, V. C., Geijtenbeek, T. B. and van Kooyk, Y.**, The C-type lectin macrophage galactose-type lectin impedes migration of immature APCs. *J. Immunol.* 2008. **181**: 3148–3155.

7 **van Vliet, S. J., van Liempt, E., Saeland, E., Aarnoudse, C. A., Appelmelk, B., Irimura, T., Geijtenbeek, T. B. et al.**, Carbohydrate profiling reveals a distinctive role for the C-type lectin MGL in the recognition of helminth parasites and tumor antigens by dendritic cells. *Int. Immunol.* 2005. **17**: 661–669.

8 **Tsuiji, M., Fujimori, M., Ohashi, Y., Higashi, N., Onami, T. M., Hedrick, S. M. and Irimura, T.**, Molecular cloning and characterization of a novel mouse macrophage C-type lectin, mMGL2, which has a distinct carbohydrate specificity from mMGL1. *J. Biol. Chem.* 2002. **277**: 28892–28901.

9 **Kumamoto, Y., Denda-Nagai, K., Aida, S., Higashi, N. and Irimura, T.**, MGL2 Dermal dendritic cells are sufficient to initiate contact hypersensitivity in vivo. *PLoS One* 2009. **4**: e5619.

10 **Singh, S. K., Streng-Ouwehand, I., Litjens, M., Weelij, D. R., García-Vallejo, J. J., van Vliet, S. J., Saeland, E. et al.**, Characterization of murine MGL1 and MGL2 C-type lectins: distinct glycan specificities and tumor binding properties. *Mol. Immunol.* 2009. **46**: 1240–1249.

11 **van Vliet, S. J., Aarnoudse, C. A., Broks-van den Berg, V. C., Boks, M., Geijtenbeek, T. B. and van Kooyk, Y.**, MGL-mediated internalization and antigen presentation by dendritic cells: a role for tyrosine-5. *Eur. J. Immunol.* 2007. **37**: 2075–2081.

12 **Takada, A., Fujioka, K., Tsuiji, M., Morikawa, A., Higashi, N., Ebihara, H., Kobasa, D. et al.**, Human macrophage C-type lectin specific for galactose and N-acetylgalactosamine promotes filovirus entry. *J. Virol.* 2004. **78**: 2943–2947.

13 **van Liempt, E., van Vliet, S. J., Engering, A., García Vallejo, J. J., Bank, C. M., Sanchez-Hernandez, M., van Kooyk, Y. et al.**, Schistosoma mansoni soluble egg antigens are internalized by human dendritic cells through multiple C-type lectins and suppress TLR-induced dendritic cell activation. *Mol. Immunol.* 2007. **44**: 2605–2615.

14 **van Sorge, N. M., Bleumink, N. M., van Vliet, S. J., Saeland, E., van der Pol, W. L., van Kooyk, Y. and van Putten, J. P.**, N-glycosylated proteins and distinct lipooligosaccharide glycoforms of Campylobacter jejuni target the human C-type lectin receptor MGL. *Cell. Microbiol.* 2009. **11**: 1768–1781.

15 **van Vliet, S. J., Steeghs, L., Bruijns, S. C., Vaezirad, M. M., Snijders Blok, C., Arenas Busto, J. A., Deken, M. et al.**, Variation of *Neisseria gonorrhoeae* lipooligosaccharide directs dendritic cell-induced T helper responses. *PLoS Pathog.* 2009. **5**: e1000625.

16 **van Vliet, S. J., Gringhuis, S. I., Geijtenbeek, T. B. and van Kooyk, Y.**, Regulation of effector T cells by antigen-presenting cells via

interaction of the C-type lectin MGL with CD45. *Nat. Immunol.* 2006. **7**: 1200–1208.

17 **Saeland, E., van Vliet, S. J., Bäckström, M., van den Berg, V. C., Geijtenbeek, T. B., Meijer, G. A. and van Kooyk, Y.**, The C-type lectin MGL expressed by dendritic cells detects glycan changes on MUC1 in colon carcinoma. *Cancer Immunol. Immunother.* 2007. **56**: 1225–1236.

18 **Napoletano, C., Rughetti, A., Agervig Tarp, M. P., Coleman, J., Bennett, E. P., Picco, G., Sale, P. et al.**, Tumor-associated Tn-MUC1 glycoform is internalized through the macrophage galactose-type C-type lectin and delivered to the HLA class I and II compartments in dendritic cells. *Cancer Res.* 2007. **67**: 8358–8367.

19 **Gendler, S. J., Spicer, A. P., Lalani, E. N., Duhig, T., Peat, N., Burchell, J., Pemberton, L. et al.**, Structure and biology of a carcinoma-associated mucin, MUC1. *Am. Rev. Respir. Dis.* 1991. **144**: S42–S47.

20 **Burchell, J. M., Mungul, A. and Taylor-Papadimitriou, J.**, O-linked glycosylation in the mammary gland: changes that occur during malignancy. *J. Mammary Gland Biol. Neoplasia* 2001. **6**: 355–364.

21 **Kaisho, T. and Tanaka, T.**, Turning NF-kappaB and IRFs on and off in DC. *Trends Immunol.* 2008. **29**: 329–336.

22 **Nishikori, M.**, Classical and alternative NfkB activation pathways and their roles in lymphoid malignancies. *J. Clin. Exp. Hematopathol.* 2005. **45**: 15–22.

23 **Ouaaz, F., Arron, J., Zheng, Y., Choi, Y. and Beg, A. A.**, Dendritic cell development and survival require distinct NF-kappaB subunits. *Immunity* 2002. **16**: 257–270.

24 **Nakahara, T., Moroi, Y., Uchi, H. and Furue, M.**, Differential role of MAPK signaling in human dendritic cell maturation and Th1/Th2 engagement. *J. Dermatol. Sci.* 2006. **42**: 1–11.

25 **Sallusto, F., Cella, M., Danieli, C. and Lanzavecchia, A.**, Dendritic cells use macropinocytosis and the mannose receptor to concentrate macromolecules in the major histocompatibility complex class II compartment: downregulation by cytokines and bacterial products. *J. Exp. Med.* 1995. **182**: 389–400.

26 **Scott, K., Manunta, M., Germain, C., Smith, P., Jones, M., Mitchell, P., Dessi, D. et al.**, Qualitatively distinct patterns of cytokines are released by human dendritic cells in response to different pathogens. *Immunology* 2005. **116**: 245–254.

27 **Simon, T., Fonteneau, J. F. and Grégoire, M.**, Dendritic cell preparation for immunotherapeutic interventions. *Immunotherapy* 2009. **1**: 289–302.

28 **Unger, W. W. and van Kooyk, Y.**, "Dressed for success" C-type lectin receptors for the delivery of glyco-vaccines to dendritic cells. *Curr. Opin. Immunol.* 2011. **23**: 131–137.

29 **Freire, T., Zhang, X., Dériaud, E., Ganneau, C., Vichier-Guerre, S., Azria, E., Launay, O. et al.**, Glycosidic Tn-based vaccines targeting dermal dendritic cells favor germinal center B-cell development and potent antibody response in the absence of adjuvant. *Blood* 2010. **116**: 3526–3536.

30 **Singh, S. K., Streng-Ouwehand, I., Litjens, M., Kalay, H., Saeland, E. and van Kooyk, Y.**, Tumour-associated glycan modifications of antigen enhance MGL2 dependent uptake and MHC class I restricted CD8 T cell responses. *Int. J. Cancer* 2011. **128**: 1371–1383.

31 **Denda-Nagai, K., Aida, S., Saba, K., Suzuki, K., Moriyama, S., Oo-Puthinan, S., Tsuiji, M. et al.**, Distribution and function of macrophage galactose-type C-type lectin 2 (MGL2/CD301b): efficient uptake and presentation of glycosylated antigens by dendritic cells. *J. Biol. Chem.* 2010. **285**: 19193–19204.

32 **Ni, L., Gayet, I., Zurawski, S., Duluc, D., Flamar, A. L., Li, X. H., O'Bar, A. et al.**, Concomitant activation and antigen uptake via human dectin-1 results in potent antigen-specific CD8+ T cell responses. *J. Immunol.* 2010. **185**: 3504–3513.

33 **Caparrós, E., Munoz, P., Sierra-Filardi, E., Serrano-Gómez, D., Puig-Kröger, A., Rodríguez-Fernández, J. L., Mellado, M. et al.**, DC-SIGN ligation on dendritic cells results in ERK and PI3K activation and modulates cytokine production. *Blood* 2006. **107**: 3950–3958.

34 **Singh, S. K., Streng-Ouwehand, I., Litjens, M., Kalay, H., Burgdorf, S., Saeland, E., Kurts, C. et al.**, Design of neo-glycoconjugates that target the mannose receptor and enhance TLR-independent cross-presentation and Th1 polarization. *Eur. J. Immunol.* 2011. **41**: 916–925.

35 **Sartorius, R., Bettua, C., D'Apice, L., Caivano, A., Trovato, M., Russo, D., Zanoni, I. et al.**, Vaccination with filamentous bacteriophages targeting DEC-205 induces DC maturation and potent anti-tumor T-cell responses in the absence of adjuvants. *Eur. J. Immunol.* 2011. **41**: 2573–2584.

36 **Idoyaga, J., Cheong, C., Suda, K., Suda, N., Kim, J. Y., Lee, H., Park, C. G. et al.**, Cutting edge: langerin/CD207 receptor on dendritic cells mediates efficient antigen presentation on MHC I and II products in vivo. *J. Immunol.* 2008. **180**: 3647–3650.

37 **Flacher, V., Tripp, C. H., Stoitzner, P., Haid, B., Ebner, S., Del Frari, B., Koch, F. et al.**, Epidermal Langerhans cells rapidly capture and present antigens from C-type lectin-targeting antibodies deposited in the dermis. *J. Invest. Dermatol.* 2010. **130**: 755–762.

38 **Caux, C., Vanbervliet, B., Massacrier, C., Azuma, M., Okumura, K., Lanier, L. L. and Banchereau, J.**, B70/B7–2 Is Identical to CD86 and Is the Major Functional Ligand for CD28 Expressed on Human Dendritic Cells. *J. Exp. Med.* 1996. **180**: 1841–1847.

39 **Puig-Kröger, A., Relloso, M., Fernández-Capetillo, O., Zubiaga, A., Silva, A., Bernabéu, C. and Corbi,' A.L.**, Extracellular signal-regulated protein kinase signaling pathway negatively regulates the phenotypic and functional maturation of monocyte-derived human dendritic cells. *Blood* 2001. **98**: 2175–2182.

40 **Ardeshna, K. M., Pizzey, A. R., Devereux, S. and Khwaja, A.**, The PI3 kinase, p38 SAP kinase, and NF-kappaB signal transduction pathways are involved in the survival and maturation of lipopolysaccharide-stimulated human monocyte-derived dendritic cells. *Blood* 2000. **96**: 1039–1046.

41 **Palucka, K., Ueno, H. and Banchereau, J.**, Recent developments in cancer vaccines. *J. Immunol.* 2001. **186**: 1325–1331.

42 **Fontenot, J. D., Finn, O. J., Dales, N., Andrews, P. C. and Montelaro, R. C.**, Synthesis of large multideterminant peptide immunogens using a poly-proline beta-turn helix motif. *Pept. Res.* 1993. **6**: 330–336.

43 **Wandall, H. H., Hassan, H., Mirgorodskaya, E., Kristensen, A. K., Roepstorff, P., Bennett, E. P., Nielsen, P. A. et al.**, Substrate specificities of three members of the human UDP-N-acetyl-alpha-D-galactosamine: polypeptide N-acetylgalactosaminyltransferase family, GalNAc-T1, -T2, and -T3. *J. Biol. Chem.* 1997. **272**: 23503–23514.

Abbreviations: **a-MGL-DC**: anti-MGL antibody treated DC · **CLR**: C-type lectin receptor · **GalNAc or Tn**: α-N-acetylgalactosamine · **hMGL**: human MGL · **iDC**: immature DC · **mDC**: mature DC · **MFI**: mean fluorescence intensity · **MGL**: macrophage galactose-type C-type lectin · **MUC1$_{9Tn}$**: MUC1 peptide carrying 9Tn moles · **RT**: room temperature · **TAA**: tumor-associated antigen · **TR**: tandem repeat

Full correspondence: Prof. Marianna Nuti, Department of Experimental Medicine, "Sapienza" University of Rome, Viale Regina Elena 324, 00161 Rome, Italy
Fax: +390-64997-3029
e-mail: marianna.nuti@uniroma1.it

Received: 5/9/2011
Revised: 11/11/2011
Accepted: 22/12/2011
Accepted article online: 4/1/2012

